

macromolecules by complexation with β -CD is probably due to intermacromolecular chemical cross-linking by the MPC polymer chains. The CM nanogels have a dual cross-linking structure that is physically cross-linked with the cholesteryl groups and chemically cross-linked with the MPC polymer chains.

Interaction of Hybrid Nanogels with Proteins

It is important to trap proteins in hydrogels without their aggregations and to control release of proteins in a native form for developing effective protein reservoirs in drug delivery systems and artificial molecular chaperones in biotechnology. Irreversible adsorption of proteins is sometimes unavoidable in trapping them in the hydrogels because it is generally difficult to control the mesh size of the hydrogel matrix and also the cross-linking sites. We previously reported that even denatured proteins that were trapped in the nanogels without aggregations can be refolded to intact forms after being released from the nanogels and are therefore useful as artificial chaperones^[8,10] or drug carriers.^[9] In this study, we investigated whether the ability to trap and release proteins by the addition of cyclodextrin (CD) remains after conjugation of the MPC polymers and chemical cross-linking. The results also provide important insights into the cross-linking structure of the nanogels.

Carbonic anhydrase B (CAB) was selected as a model enzyme. CAB aggregated and precipitated after being heated at 70 °C for 10 min. In this process, exposure of the hydrophobic surface of the heat-denatured protein results in irreversible aggregation. In the presence of hybrid nanogels, however, the solution was transparent even after heating under the same conditions. This phenomenon is caused by the complexation of the denatured CAB with the hybrid nanogels. The enzyme activity of the complex was lost by trapping denatured protein (enzyme activity of the complex, CM6 nanogels: $5.0 \pm 0.2\%$, CM14 nanogels: $5.7 \pm 0.5\%$, CHP nanogels: $5.0 \pm 0.1\%$). Hydrophobic interaction between the hydrophobic domain of the cholesteryl group in the nanogels and the exposed hydrophobic surface of the denatured protein plays an important role in the complexation. CM nanogels retain their activity of trapping heat-denatured protein.

Both complexes, CM6-CAB and CM14-CAB, were stable under this condition. No protein release from the complexes was observed at 20 °C for at least 24 h in the absence of β -CD. In the presence of β -CD, however, dissociation of the hydrophobic domain in the nanogels subsequently induced the release of the proteins as well as protein refolding, as previously reported.^[8,10] Two hours after the addition of β -CD, enzyme activity recovered in both the CM6 and CM14 nanogel systems (CM6 nanogels: $66.8 \pm 1.1\%$, CM14 nanogels: $59.1 \pm 1.5\%$, CHP nanogels: $62.8 \pm 4.8\%$). The activity of the hybrid nanogels is comparable to that of the CHP nanogels. The results show that the

complexation of nanogels with protein or β -CD effectively occurs even in the chemical cross-linking of the nanogels. Chemical cross-linking and surface coating by such MPC polymers did not affect the trapping and release of the protein because the hydrophobic association by physically cross-linked domains of the cholesteryl groups is important in the interaction of proteins with nanogels. In addition, the MPC polymers of the hybrid nanogels act as a suitable inert matrix for the trapped proteins due to the reduction of protein adsorption.^[19] This property is essential for the application of hybrid nanogels in DDS and to artificial molecular chaperone as well as to the improved colloidal stability of nanogels by the surface coating of the MPC polymers. Based on the results, application of hybrid nanogels in DDS is now under investigation in our laboratory.

Conclusion

Monodispersed hybrid nanogels were successfully prepared by using seed-nanogels with polymerizable groups. The hybrid nanogels exhibited the ability of trapping denatured CAB and then releasing CAB in its native form. A variety of monodispersed functional nanogels can be designed by selecting various self-assembled nanogels as seeds and by selecting various functional monomers. Such hybrid nanogels are useful for applications in biotechnology and drug delivery systems.

Acknowledgements: This work was supported by a Grant-in-Aid for Scientific Research from the *Japanese Government* (No. 17300147). K. A. acknowledges the financial support from *Sekisui Chemical Co. Ltd.*

- [1] [1a] J. Kopecek, *Nature* **2002**, *417*, 388; [1b] M. E. Byrne, K. Park, N. A. Peppas, *Adv. Drug Delivery Rev.* **2002**, *54*, 149.
- [2] [2a] S. V. Vinogradov, T. K. Bronich, A. V. Kabanov, *Adv. Drug Delivery Rev.* **2002**, *54*, 135; [2b] K. McAllister, P. Sazani, M. Adam, M. J. Cho, M. Rubinstein, R. J. Samulski, J. M. DeSimone, *J. Am. Chem. Soc.* **2002**, *124*, 15198.
- [3] D. Gan, L. A. Lyon, *J. Am. Chem. Soc.* **2001**, *123*, 7511.
- [4] [4a] D. Kuckling, C. D. Vo, S. E. Wohlrab, *Langmuir* **2002**, *18*, 4263; [4b] J. Zhou, Z. Li, G. Liu, *Macromolecules* **2002**, *35*, 3690.
- [5] [5a] K. B. Thumond II, T. Kowalewski, K. L. Wooley, *J. Am. Chem. Soc.* **1996**, *118*, 7239; [5b] V. Büttin, N. C. Billingham, S. P. Armes, *J. Am. Chem. Soc.* **1998**, *120*, 12135; [5c] H. Hayashi, M. Iijima, K. Kataoka, Y. Nagasaki, *Macromolecules* **2004**, *37*, 5389.
- [6] [6a] K. Akiyoshi, S. Deguchi, N. Moriguchi, S. Yamaguchi, J. Sunamoto, *Macromolecules* **1993**, *26*, 3062; [6b] K. Akiyoshi, S. Deguchi, H. Tajima, T. Nishikawa, J. Sunamoto, *Macromolecules* **1997**, *30*, 857; [6c] K. Akiyoshi, J. Sunamoto, *Supramolecular Sci.* **1996**, *3*, 157.

- [7] [7a] T. Nishikawa, K. Akiyoshi, J. Sunamoto, *J. Am. Chem. Soc.* **1996**, *118*, 6110; [7b] T. Nishikawa, K. Akiyoshi, J. Sunamoto, *Macromolecules* **1994**, *27*, 7654.
- [8] K. Akiyoshi, Y. Sasaki, J. Sunamoto, *Bioconjugate Chem.* **1999**, *10*, 321.
- [9] [9a] K. Akiyoshi, S. Kobayashi, S. Shichibe, D. Mix, M. Baudys, S. W. Kim, J. Sunamoto, *J. Controlled Release* **1998**, *54*, 313; [9b] Y. Ikuta, N. Katayama, L. Wang, T. Okugawa, Y. Takahashi, M. Schmitt, X. Gu, M. Watanabe, K. Akiyoshi, H. Nakamura, K. Kuribayashi, J. Sunamoto, H. Shiku, *Blood* **2002**, *99*, 3717; [9c] X-G. Gu, M. Schmitt, A. Hiasa, Y. Nagata, H. Ikeda, Y. Sasaki, K. Akiyoshi, J. Sunamoto, H. Nakamura, K. Kuribayashi, H. Shiku, *Cancer Res.* **1998**, *58*, 3385.
- [10] Y. Nomura, M. Ikeda, N. Yamaguchi, Y. Aoyama, K. Akiyoshi, *FEBS Lett.* **2003**, *553*, 271.
- [11] K. Akiyoshi, A. Ueminami, S. Kurumada, Y. Nomura, *Macromolecules* **2000**, *33*, 6752.
- [12] K. Akiyoshi, E.-C. Kang, S. Kurumada, J. Sunamoto, T. Principi, F. M. Winnik, *Macromolecules* **2000**, *33*, 3244.
- [13] T. Hirakura, Y. Nomura, Y. Aoyama, K. Akiyoshi, *Biomacromolecules* **2004**, *5*, 1804.
- [14] [14a] K. Y. Lee, W. H. Jo, *Langmuir* **1998**, *14*, 2329; [14b] K. Y. Lee, W. H. Jo, I. C. Kwon, Y. Kim, S. Y. Jeong, *Macromolecules* **1998**, *31*, 378.
- [15] M. Nichifor, A. Lopes, A. Carpov, E. Melo, *Macromolecules* **1999**, *32*, 7078.
- [16] S. Yusa, M. Kamachi, Y. Morishima, *Langmuir* **1998**, *14*, 6059.
- [17] K. Akiyoshi, I. Taniguchi, H. Fukui, J. Sunamoto, *Eur. J. Pharm. Biopharm.* **1996**, *42*, 286.
- [18] I. Taniguchi, M. Fujiwara, K. Akiyoshi, J. Sunamoto, *Bull. Chem. Soc. Jpn.* **1998**, *71*, 2681.
- [19] [19a] K. Ishihara, T. Ueda, N. Nakabayashi, *Polym. J.* **1990**, *22*, 355; [19b] K. Ishihara, H. Nomura, T. Mihara, K. Kurita, Y. Iwasaki, N. Nakabayashi, *J. Biomed. Mater. Res.* **1998**, *39*, 323; [19c] T. Konno, K. Kurita, Y. Iwasaki, N. Nakabayashi, K. Ishihara, *Biomaterials* **2001**, *22*, 1883.
- [20] T. Konno, K. Ishihara, *Trans. Mater. Res. Soc. Jpn.* **2001**, *26*, 897.
- [21] N. Morimoto, T. Endo, Y. Iwasaki, K. Akiyoshi, *Biomacromolecules* **2005**, *6*, 1809.
- [22] K. Akiyoshi, S. Sasaki, K. Kuroda, J. Sunamoto, *Chem. Lett.* **1998**, 93.
- [23] R. Breslow, B. J. Zhang, *J. Am. Chem. Soc.* **1996**, *118*, 8495.

Leading Opinion

How useful is SBF in predicting in vivo bone bioactivity? ☆

Tadashi Kokubo*, Hiroaki Takadama

Department of Biomedical Sciences, College of Life and Health Sciences, Chubu University, 1200 Matsumoto, Kasugai, Aichi 487-8501, Japan

Received 6 September 2005; accepted 13 January 2006

Available online 31 January 2006

Abstract

The bone-bonding ability of a material is often evaluated by examining the ability of apatite to form on its surface in a simulated body fluid (SBF) with ion concentrations nearly equal to those of human blood plasma. However, the validity of this method for evaluating bone-bonding ability has not been assessed systematically. Here, the history of SBF, correlation of the ability of apatite to form on various materials in SBF with their in vivo bone bioactivities, and some examples of the development of novel bioactive materials based on apatite formation in SBF are reviewed. It was concluded that examination of apatite formation on a material in SBF is useful for predicting the in vivo bone bioactivity of a material, and the number of animals used in and the duration of animal experiments can be reduced remarkably by using this method.

© 2006 Elsevier Ltd. All rights reserved.

Keywords: Bioactivity; Bone; Hydroxyapatite; In vitro test; Osteoconduction; SBF

1. Introduction

Artificial materials implanted into bone defects are generally encapsulated by a fibrous tissue, leading to their isolation from the surrounding bone. However, in 1972, Hench et al. showed that some glasses in the Na_2O – CaO – SiO_2 – P_2O_5 system, called Bioglass, spontaneously bond to living bone without the formation of surrounding fibrous tissue [1]. Since then, several types of ceramic, such as sintered hydroxyapatite [2], sintered β -tricalcium phosphate [3], apatite/ β -tricalcium phosphate biphasic ceramics [4], and glass-ceramic A–W containing crystalline apatite and wollastonite [5] have been also shown to bond to living bone, and they are used clinically as important bone substitutes. However, these ceramics are not compatible

mechanically to the surrounding bone. The development of bone-bonding materials with different mechanical properties is desired.

This desire leads to two questions: what type of material bonds to living bone; and are animal experiments the only one way to test for bone bonding, that is, to identify a material with in vivo bone bioactivity? In 1991, we proposed that the essential requirement for an artificial material to bond to living bone is the formation of bonelike apatite on its surface when implanted in the living body, and that this in vivo apatite formation can be reproduced in a simulated body fluid (SBF) with ion concentrations nearly equal to those of human blood plasma [6]. This means that the in vivo bone bioactivity of a material can be predicted from the apatite formation on its surface in SBF. Since then, in vivo bone bioactivity of various types of materials have been evaluated by apatite formation in SBF. However, the validity of this method has not been systematically assessed.

Here, the history of SBF, correlation of the ability of apatite to form on various materials in SBF with their in vivo bone bioactivities, and some examples of successful development of novel bioactive materials based on the apatite formation on their surfaces in SBF are reviewed.

☆ *Editor's Note:* Leading Opinions: This paper is one of a newly instituted series of scientific articles that provide evidence-based scientific opinions on topical and important issues in biomaterials science. They have some features of an invited editorial but are based on scientific facts, and some features of a review paper, without attempting to be comprehensive. These papers have been commissioned by the Editor-in-Chief and reviewed for factual, scientific content by referees.

*Corresponding author. Tel: +81 568 51 6583; fax: +81 568 51 1642.

E-mail address: kokubo@isc.chubu.ac.jp (T. Kokubo).

2. History of SBF

In 1980, Hench et al. showed that a SiO₂-rich layer and calcium phosphate film form on the surface of Bioglass when implanted in the body environment, which allows bonding to living bone, and that the *in vivo* formation of the calcium phosphate film can be reproduced in a buffer solution consisting of Tris hydroxymethylaminomethane and hydrochloric acid (Tris buffer solution) at pH 7.4 [7].

On the other hand, Kitsugi et al. showed that the SiO₂-rich layer does not form on glass-ceramic A–W, but a calcium phosphate layer forms on its surface in the living body, allowing bonding to living bone [8]. Subsequently, Kokubo et al., using micro X-ray diffraction, identified this calcium phosphate layer as crystalline apatite [9]. In addition, in 1990, they showed that the *in vivo* apatite formation on the surface of glass-ceramic A–W can be reproduced in an acellular SBF with ion concentrations nearly equal to those of the human blood plasma, but not in a Tris buffer solution [10,11]. Kokubo et al. [10] and Hench et al. [12] also independently confirmed the formation of apatite on the surface of Bioglass 45S5-type glass in SBF.

Detailed analysis of the surface apatite formed in SBF, by means of thin film X-ray diffraction (TF-XRD), Fourier transform infrared spectroscopy, scanning electron microscopy and transmission electron microscopy, showed that it was similar to bone mineral in its composition and structure [10,11,13]. As a result, it was speculated that osteoblasts might preferentially proliferate and differentiate to produce apatite and collagen on its surface. Thus formed apatite might bond to the surface apatite as well as to the surrounding bone. Consequently, a tight chemical bond is formed between the material and the living bone through the apatite layer. In contrast, glass-ceramic A–W (Al), which also contains apatite and wollastonite, but in a glassy matrix containing Al₂O₃, and hence does not bond to living bone, did not have apatite form on its surface, both *in vivo* and in SBF [11,14]. Based on these results, in 1991 it was proposed that the essential requirement for a material to bond to living bone is the formation of bonelike apatite on its surface in the living body and that this *in vivo* apatite formation can be reproduced in SBF. This means that the *in*

vivo bone bioactivity of a material can be predicted by examining apatite formation on its surface in SBF [6].

It should be noted here that the original SBF used by Kokubo et al. [10] and Hench et al. [12] lacks the SO₄²⁺ ions contained in human blood plasma [15], as shown in Table 1. This was corrected in papers [6,16] published by Kokubo et al. in 1991. Since then, the corrected SBF has been used as “SBF” by many researchers.

It should be also noted here that SBF is a solution highly supersaturated with respect to apatite [17]. It is not easy to prepare clear SBF with no precipitation. Therefore, a detailed recipe for preparation of SBF was reported in 1995 by Cho et al. [18].

However, it can be seen from Table 1 that corrected SBF is still richer in Cl[−] ion and poorer in HCO₃[−] ion than human blood plasma. In 2003, Oyane et al. tried to correct this difference [19] by preparing a revised SBF (r-SBF) in which the concentrations of Cl[−] and HCO₃[−] ions were, decreased and increased respectively, to the levels of human blood plasma. However, calcium carbonate has a strong tendency to precipitate from this SBF, as it is supersaturated with respect to not only apatite, but also calcite [20]. In 2004, Takadama et al. proposed a newly improved SBF (n-SBF) in which they decreased only the Cl[−] ion concentration to the level of human blood plasma, leaving the HCO₃[−] ion concentration equal to that of the corrected SBF (c-SBF) [21]. This improved SBF was compared with the corrected, i.e., conventional, c-SBF in its stability and the reproducibility of apatite formation on synthetic materials. Both SBFs were subjected to round robin testing in ten research institutes. As a result, it was confirmed that the c-SBF does not differ from n-SBF in stability and reproducibility [21]. Through this round robin testing, the method for preparing c-SBF was carefully checked and refined so that the SBF could be easily prepared. This refined recipe for preparing SBF is given in Appendix A of this paper, accompanied with procedure of apatite-forming ability test.

In 2003, conventional SBF with the refined recipe was proposed to the Technical Committee ISO/TC150 of International Organization for Standardization as a solution for *in vitro* measurement of apatite-forming ability of implant materials and is being discussed by the committee.

Table 1
Ion concentrations of SBFs and human blood plasma

	Ion concentration (mM)							
	Na ⁺	K ⁺	Mg ²⁺	Ca ²⁺	Cl [−]	HCO ₃ [−]	HPO ₄ ^{2−}	SO ₄ ^{2−}
Human blood plasma [15]	142.0	5.0	1.5	2.5	103.0	27.0	1.0	0.5
Original SBF	142.0	5.0	1.5	2.5	148.8	4.2	1.0	0
Corrected SBF (c-SBF)	142.0	5.0	1.5	2.5	147.8	4.2	1.0	0.5
Revised SBF (r-SBF)	142.0	5.0	1.5	2.5	103.0	27.0	1.0	0.5
Newly improved SBF (n-SBF)	142.0	5.0	1.5	2.5	103.0	4.2	1.0	0.5

3. Qualitative correlation of apatite formation in SBF with in vivo bone bioactivity

As described above, a glass in the Na_2O – CaO – SiO_2 – P_2O_5 system named Bioglass 45S5 has apatite form on its surface in SBF [10]. This glass was confirmed to bond to living bone through a calcium phosphate layer [7]. Glasses in the Na_2O – CaO – B_2O_3 – Al_2O_3 – SiO_2 – P_2O_5 system were also found to have a calcium phosphate layer form on their surfaces in SBF [22]. These glasses were also confirmed to bond to living bone through a calcium phosphate layer in vivo [22].

Ceravital®-type glass-ceramic containing apatite was also found to form apatite on its surface in SBF [16] and was confirmed to bond to living bone through a calcium phosphate layer in vivo [16]. Glass-ceramic A–W forms apatite on its surface in SBF, as shown in Fig. 1 [11] and Fig. 2 [13], and was confirmed to bond to living bone through the apatite layer in vivo, as shown in Fig. 3 [9,23]. In contrast, as described above, glass-ceramic A–W (Al) does not form an apatite layer on its surface in SBF [11], does not have apatite form on its surface in vivo and does not bond to living bone [14]. The apatite forming ability of Bioverite®-type glass-ceramic containing apatite and phlogopite has not been examined in SBF, but it has been confirmed to bond to living bone through a calcium phosphate layer [24].

Sintered hydroxyapatite was also found to have apatite form on its surface in SBF [25,26] and was confirmed to bond to living bone through an apatite layer in vivo [23]. Apatite/ β -tricalcium phosphate biphasic ceramic was also found to have an apatite layer form on its surface in SBF [4] and was confirmed to bond to living bone through the apatite layer in vivo [4]. Calcium sulfate was also found to form an apatite on its surface in SBF as well as in vivo [27].

For composites, a composite in which glass-ceramic A–W particles are dispersed in a polyethylene matrix was also found to have apatite form on its surface in SBF [28] and bonded to living bone [29]. For all these materials, apatite formation on their surfaces in SBF is well correlated with their in vivo bone bioactivities.

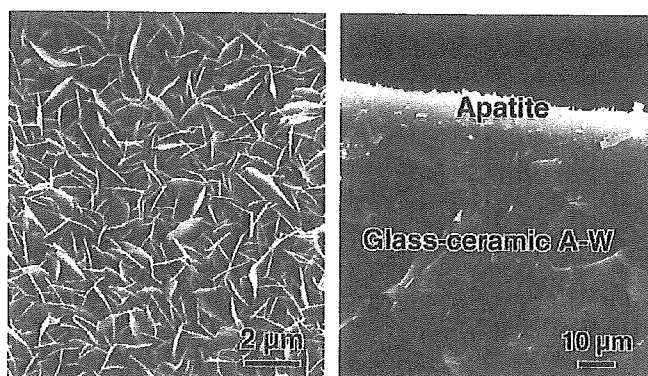


Fig. 1. Scanning electron micrograph of surface (left) and cross section (right) of apatite layer formed on glass-ceramic A–W in SBF [11].

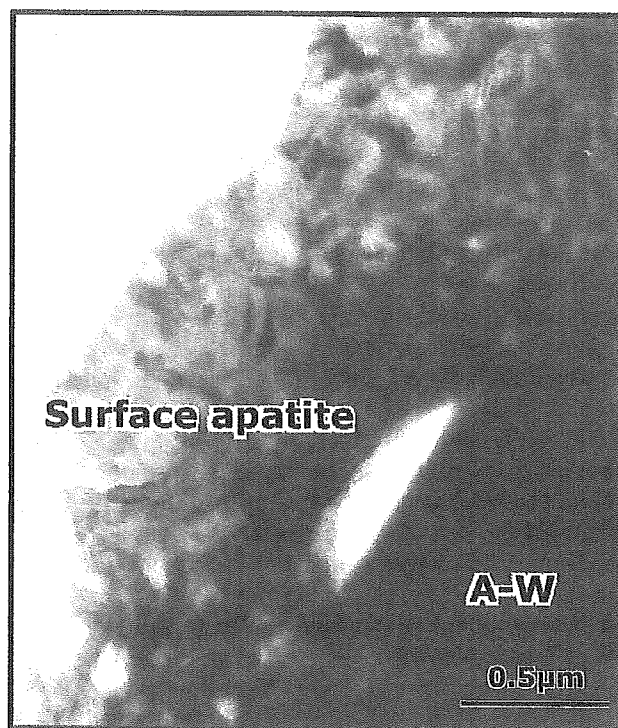


Fig. 2. Transmission electron micrograph of cross section of apatite layer formed on glass-ceramic A–W in SBF [13].

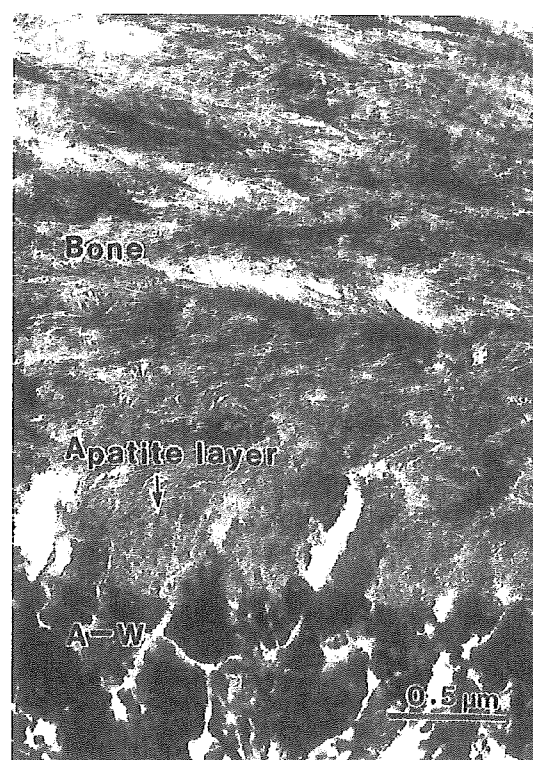


Fig. 3. Transmission electron micrograph of interface between glass-ceramic A–W and rat tibia [23].

However, both β -tricalcium phosphate and natural calcite do not have apatite form on their surfaces in SBF [30,31] or in vivo. [32–34], but despite this, they bond to living bone [32–34]. These results might be related to the high resorbability of these materials. In contrast, natural abalone shell has apatite form on its surface in SBF [31], but does not bond to living bone [35], which might be attributed to antibody reactions to proteins in the shell.

In some reports, SBF with ion concentrations 1.5 times those of SBF (1.5 SBF) has been used when evaluating the in vivo bone bioactivity of a material. There is, however, no correlation between apatite formation on a material in 1.5 SBF with its in vivo bone bioactivity.

It can be said from these results that a material able to have apatite form on its surface in SBF can bond to living bone through the apatite layer formed on its surface in the living body, as long as the material does not contain any substance that induces toxic or antibody reactions.

4. Quantitative correlation of apatite formation in SBF with in vivo bone bioactivity

In 1995, Kim et al. [36] showed that P_2O_5 -free Na_2O - CaO - SiO_2 glasses of a wide compositional range have apatite form on their surfaces in SBF, and their apatite forming abilities vary largely with their compositions: i.e. the soaking time in SBF required for apatite formation on their surfaces increased from 0.5 d to longer than 28 d with SiO_2 contents increasing from 50.0 to 70.0 mol% with equal molar concentrations of Na_2O and CaO . Granular particles of these glasses were implanted into holes in rabbit tibiae. The depth of bone growth from the periphery to the interior of the holes at 3 and 6 weeks after implantation increased with the increasing apatite-forming ability of the glasses in SBF at the respective implantation times, as shown in Fig. 4 [37]. The apatite-forming abilities of hydroxyapatite (HA), glass-ceramic A-W and Bioglass in SBF is reported to increase with the order $HA < A-W < Bioglass$ [10,25]. According to Oonishi et al., the depth of bone growth from the periphery to the interior of holes filled with these materials in the tibiae of rabbit also increased in the order $HA < A-W < Bioglass$ [38].

It can be said from these results that the degree of ability for apatite to form on the surface of a material in SBF can predict the degree of in vivo bone bioactivity of the material. A material able to form apatite on its surface in SBF in a short period bonds to living bone in a short period, as a result of apatite formation on its surface in a shorter period within the living body.

5. Development of novel bioactive materials based on apatite formation in SBF

It was shown that CaO and P_2O_5 -based glasses in the system CaO - SiO_2 - P_2O_5 do not have apatite form on their surfaces in SBF, whereas it forms on CaO and SiO_2 -based

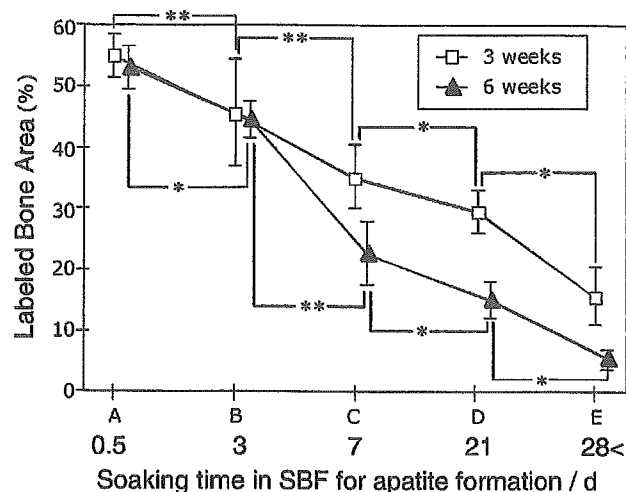


Fig. 4. Dependence of bone formation in a hole of rat tibia filled with glasses on apatite-forming ability of glasses in SBF. Apatite-forming ability increases with decreasing soaking time in SBF for apatite formation [37]. * $p < 0.05$, ** $p < 0.001$.

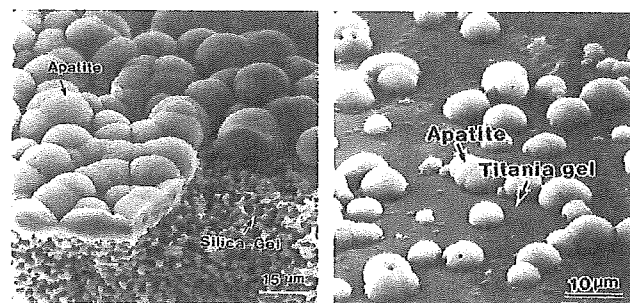


Fig. 5. Scanning electron micrograph of apatite formed on silica gel (left) and titania gel (right) in SBF [46,47].

glasses [39]. The apatite forming ability of a CaO - SiO_2 glass in SBF decreased with the addition of Fe_2O_3 to the glass, and increased with the addition of Na_2O or P_2O_5 [40]. These results then correlated well with in vivo bone bioactivity of the glasses [41,42]. Based on these results, a bioactive ferrimagnetic glass-ceramic containing magnetite in a CaO - SiO_2 -based glassy matrix was developed [43,44]. This glass-ceramic can be used as thermoseeds for hyperthermic treatment of cancer [45].

Among the metallic oxide gels prepared using a sol-gel method, those consisting of SiO_2 [46], TiO_2 [47], ZrO_2 [48], Nb_2O_5 [49] and Ta_2O_5 [50] were found to have apatite form on their surfaces in SBF, as shown in Fig. 5, but apatite did not form on gels consisting of Al_2O_3 [47]. These results indicated that $Si-OH$, $Ti-OH$, $Zr-OH$, $Nb-OH$ and $Ta-OH$ groups on the surfaces of these gels are effective for inducing apatite formation on their surfaces in the body environment.

Based on these results, it was speculated that if titanium metal, its alloys and tantalum metal form a sodium titanate or tantalate layer on their surfaces by treatment with a $NaOH$ solution and subsequent heat treatment, they could

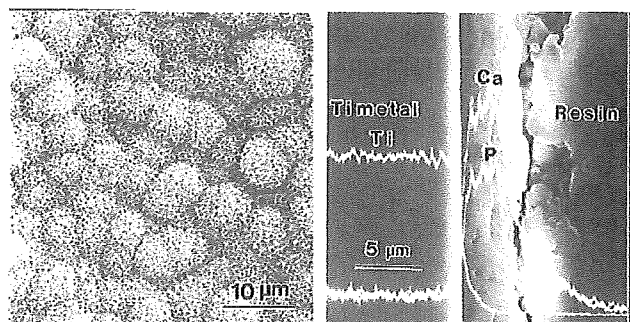


Fig. 6. Scanning electron micrograph of surface (left) and cross section (right) of apatite layer formed on NaOH- and heat-treated Ti metal in SBF [51].

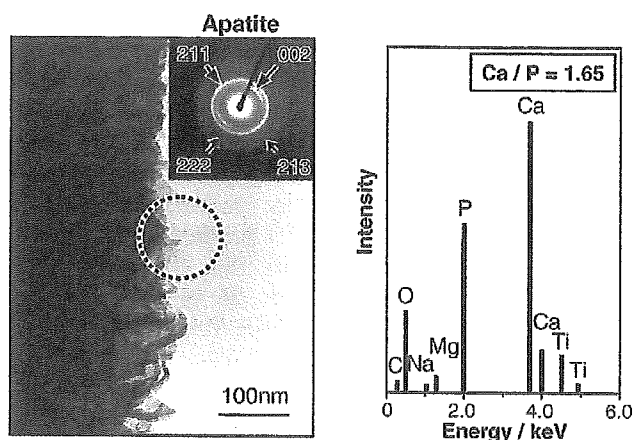


Fig. 7. Transmission electron micrograph (left) and energy dispersive X-ray spectrum (EDX) (right) of apatite formed on NaOH- and heat-treated Ti metals in SBF (dotted circle: area of electron diffraction and EDX analysis) [33].

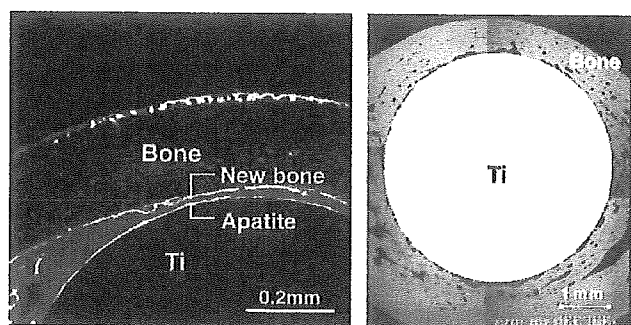


Fig. 8. Confocal laser scanning micrograph (left) and scanning electron micrograph (right) of cross section of NaOH- heat-treated Ti metal rod implanted into rabbit femur for 3 (left) and 12 (right) weeks [54].

form an apatite on their surfaces in SBF, and tightly bond to living bone through the apatite layer formed on their surfaces in the living body. Thus, treated metals had apatite form on their surfaces in SBF [51–53], as shown in Figs. 6 and 7, as well as in vivo [54,55] and, as expected, were tightly bonded to living bone, as shown in Fig. 8 [54]. The bioactive titanium metal thus developed has been applied

to artificial hip joints, and a clinical trial of 70 patients has successfully concluded.

6. Conclusion

It is apparent from the results described above that a material able to have apatite form on its surface in SBF has apatite produced on its surface in the living body, and bonds to living bone through this apatite layer. This relationship holds as long as the material does not contain a component that induces toxic or antibody reactions. There are a few materials that directly bond to living bone without the formation of detectable apatite on their surfaces. Despite this limitation, examination of apatite formation on the surface of a material in SBF is useful for predicting the in vivo bone bioactivity of the material, not only qualitatively but also quantitatively. This method can be used for screening bone bioactive materials before animal testing and the number of animals used and the duration of animal experiments can be remarkably reduced by using this method, which can assist in the efficient development of new types of bioactive materials.

Appendix A. Recipe for preparing simulated body fluid (SBF) and procedure of apatite-forming ability test

A.1. Preparation of simulated body fluid (SBF)

A.1.1. Reagents for SBF

The following powder reagent grade chemicals have to be stocked in a desiccator. Ion-exchanged and distilled water is used for the preparation of SBF:

- (1) sodium chloride (NaCl),
- (2) sodium hydrogen carbonate (NaHCO_3),
- (3) potassium chloride (KCl),
- (4) di-potassium hydrogen phosphate trihydrate ($\text{K}_2\text{HPO}_4 \cdot 3\text{H}_2\text{O}$),
- (5) magnesium chloride hexahydrate ($\text{MgCl}_2 \cdot 6\text{H}_2\text{O}$),
- (6) calcium chloride (CaCl_2),
- (7) sodium sulfate (Na_2SO_4),
- (8) Tris-hydroxymethyl aminomethane: $((\text{HOCH}_2)_3\text{CNH}_2)$ (Tris),
- (9) 1M (mol/l) Hydrochloric Acid, 1M-HCl,
- (10) pH standard solution, (pH 4, 7 and 9).

A.1.2. Ion concentrations of SBF

The ion concentrations of SBF are shown in Table A1.

A.1.3. Preparation procedure of SBF

Since SBF is supersaturated with respect to apatite, an inappropriate preparation method can lead to the precipitation of apatite in the solution. Always make sure that the preparing solution is kept colorless and transparent and that there is no deposit on the surface of the bottle. If any precipitation occurs, stop preparing SBF, abandon the

solution, restart from washing the apparatus and prepare SBF again.

In order to prepare 1000 ml of SBF, first of all, put 700 ml of ion-exchanged and distilled water with a stirring bar into 1000 ml plastic beaker. Set it in the water bath on the magnetic stirrer and cover it with a watch glass or plastic wrap. Heat the water in the beaker to $36.5 \pm 1.5^\circ\text{C}$ under stirring.

Dissolve only the reagents of 1st to 8th order into the solution at $36.5 \pm 1.5^\circ\text{C}$ one by one in the order given in Table A2, taking care of the indications in the following list. The reagents of 9th (Tris) and 10th order (small amount of HCl) are dissolved in the following process of pH adjustment:

- In preparation of SBF, glass containers should be avoided, but a plastic container with smooth surface and without any scratches is recommended, because apatite nucleation can be induced at the surface of a glass container or the edge of scratches. If the container has scratches, replace it by a new one.
- Never dissolve several reagents simultaneously. Dissolve a reagent only after the preceding one (if any) is completely dissolved.
- Since the reagent CaCl_2 , which has great effect on precipitation of apatite, takes usually granular form

and takes much time to dissolve on granule at a time, completely dissolve one before initiation of dissolution of the next.

- Measure the volume of 1M-HCl by cylinder after washing with 1M-HCl.
- Measure the hygroscopic reagents such as KCl, $\text{K}_2\text{HPO}_4 \cdot 3\text{H}_2\text{O}$, $\text{MgCl}_2 \cdot 6\text{H}_2\text{O}$, CaCl_2 , Na_2SO_4 in as short a period as possible.

Set the temperature of the solution at $36.5 \pm 1.5^\circ\text{C}$. If the amount of the solution is smaller than 900 ml, add ion-exchanged and distilled water up to 900 ml in total.

Insert the electrode of the pH meter into the solution. Just before dissolving the Tris, the pH of the solution should be 2.0 ± 1.0 .

With the solution temperature between 35 and 38°C , preferably to $36.5 \pm 0.5^\circ\text{C}$, dissolve the reagent Tris into the solution little by little taking careful note of the pH change. After adding a small amount of Tris, stop adding it and wait until the reagent already introduced is dissolved completely and the pH has become constant; then add more Tris to raise the pH gradually. When the pH becomes 7.30 ± 0.05 , make sure that the temperature of the solution is maintained at $36.5 \pm 0.5^\circ\text{C}$. With the solution at $36.5 \pm 0.5^\circ\text{C}$, add more Tris to raise the pH to under 7.45.

Note 1: Do not add a large amount of Tris into the solution at a time, because the radical increase in local pH of the solution can lead to the precipitation of calcium phosphate. If the solution temperature is not within $36.5 \pm 0.5^\circ\text{C}$, add Tris to raise the pH to 7.30 ± 0.05 , stop adding it and wait for the solution temperature to reach $36.5 \pm 0.5^\circ\text{C}$.

Note 2: The pH shall not increase over 7.45 at $36.5 \pm 0.5^\circ\text{C}$, taking account of the pH decrease with increasing solution temperature (the pH falls about $0.05/^\circ\text{C}$ at $36.5 \pm 1.5^\circ\text{C}$).

When the pH has risen to 7.45 ± 0.01 , stop dissolving Tris, then drop 1M-HCl by syringe to lower the pH to

Table A1

Nominal ion concentrations of SBF in comparison with those in human blood plasma

Ion	Ion concentrations (mM)	
	Blood plasma	SBF
Na^+	142.0	142.0
K^+	5.0	5.0
Mg^{2+}	1.5	1.5
Ca^{2+}	2.5	2.5
Cl^-	103.0	147.8
HCO_3^-	27.0	4.2
HPO_4^{2-}	1.0	1.0
SO_4^{2-}	0.5	0.5
pH	7.2–7.4	7.40

Table A2

Order, amounts, weighing containers, purities and formula weights of reagents for preparing 1000 ml of SBF

Order	Reagent	Amount	Container	Purity (%)	Formula weight
1	NaCl	8.035 g	Weighing paper	99.5	58.4430
2	NaHCO_3	0.355 g	Weighing paper	99.5	84.0068
3	KCl	0.225 g	Weighing bottle	99.5	74.5515
4	$\text{K}_2\text{HPO}_4 \cdot 3\text{H}_2\text{O}$	0.231 g	Weighing bottle	99.0	228.2220
5	$\text{MgCl}_2 \cdot 6\text{H}_2\text{O}$	0.311 g	Weighing bottle	98.0	203.3034
6	1.0M-HCl	39 ml	Graduated cylinder	—	—
7	CaCl_2	0.292 g	Weighing bottle	95.0	110.9848
8	Na_2SO_4	0.072 g	Weighing bottle	99.0	142.0428
9	Tris	6.118 g	Weighing paper	99.0	121.1356
10	1.0M-HCl	0–5 ml	Syringe	—	—

7.42 ± 0.01 , taking care that the pH does not decrease below 7.40. After the pH has fallen to 7.42 ± 0.01 , dissolve the remaining Tris little by little until the pH has risen to ≤ 7.45 . If any Tris remains, add the 1M-HCl and Tris alternately into the solution. Repeat this process until the whole amount of Tris is dissolved keeping the pH within the range of 7.42–7.45. After dissolving the whole amount of Tris, adjust the temperature of the solution to $36.5 \pm 0.2^\circ\text{C}$. Adjust the pH of the solution by dropping 1M-HCl little by little at a pH of 7.42 ± 0.01 at $36.5 \pm 0.2^\circ\text{C}$ and then finally adjust it to 7.40 exactly at 36.5°C on condition that the rate of solution temperature increase or decrease is less than $0.1^\circ\text{C}/\text{min}$.

Remove the electrode of the pH meter from the solution, rinse it with ion-exchanged and distilled water and add the washings into the solution.

Pour the pH-adjusted solution from the beaker into 1000 ml volumetric flask. Rinse the surface of the beaker with ion-exchanged and distilled water and add the washings into the flask several times, fixing the stirring bar with a magnet as if to prevent it from falling into the volumetric flask.

Add the ion-exchanged and distilled water up to the marked line (it is not necessary to adjust exactly, because the volume becomes smaller after cooling), put a lid on the flask and close it with plastic film.

After mixing the solution in the flask, keep it in the water to cool it down to 20°C .

After the solution temperature has fallen to 20°C , add the distilled water up to the marked line.

A.1.4. Confirmation of ion concentrations of SBF

Prepared SBF should have the ion concentrations shown in Table A1. In order to confirm the ion concentrations of the SBF, chemical analysis of the SBF is recommended, because SBF is a metastable solution supersaturated with respect to apatite.

Note: It is also recommended that the apatite-forming ability of standard glasses should be examined in the prepared SBF. Chemical compositions of the standard glasses are shown in Table A3. When standard glasses A–C are soaked in SBF, an apatite layer should be detected by thin-film X-ray diffraction and/or scanning electron microscopy after soaking for 12, 24 and 120 h, respectively.

Table A3
The compositions of the standard glasses in the SiO_2 – Na_2O – CaO system

Standard glass	Composition (mol%)		
	SiO_2	Na_2O	CaO
A	50	25	25
B	55	22.5	22.5
C	60	20	20

A.1.5. Preservation of SBF

Prepared SBF should be preserved in a plastic bottle with a lid put on tightly and kept at 5 – 10°C in a refrigerator. The SBF shall be used within 30 d after preparation.

A.2. Procedure of apatite-forming ability test

A.2.1. Soaking in SBF

For dense materials, measure the specimen dimensions and calculate the surface area with an accuracy of 2 mm^2 for a thin plate.

Calculate the volume of SBF that is used for testing using the following Eq. (1):

$$V_s = S_a/10, \quad (1)$$

where V_s is the volume of SBF (ml) and S_a is the apparent surface area of specimen (mm^2).

For porous materials, the volume of SBF should be greater than the calculated V_s .

Put the calculated volume of SBF into a plastic bottle or beaker. After heating the SBF to 36.5°C a specimen should be placed in the SBF as shown in Fig. A1. The entire specimen should be submerged in the SBF.

Note: In rare cases, apatite may homogeneously precipitate in the SBF and can be deposited on the surface of a specimen. Therefore, it is recommended that the specimens be placed in the SBF as shown in Fig. A1(a) or Fig. A1(b). In case of placement as shown in Fig. A1 (b), apatite formation should be examined for the lower surface of the specimen.

After soaking at 36.5°C for different periods within 4 weeks in the SBF, take out the specimen from the SBF and gently wash it with pure water. The specimen should be dried in a desiccator without heating.

Note 1: Bone bonding materials usually form apatite on their surfaces within 4 weeks.

Note 2: A specimen, once taken out of SBF and dried, should not be soaked again.

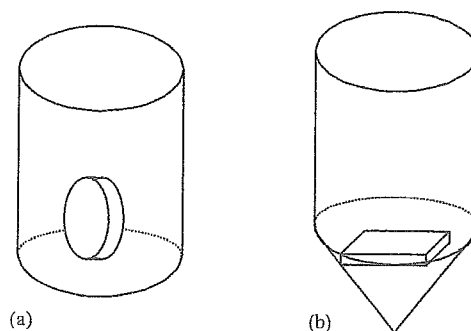


Fig. A1. A specimen in the SBF (Examples).

A.2.2. Surface characterization

Examine the surface of a specimen by TF-XRD and/or scanning electron microscope (SEM) until apatite is detected.

Note 1: The TF-XRD measurement is to be performed in the range of 3–50° in 2 theta (θ) using $\text{CuK}\alpha$ ($\lambda = 0.15405\text{ nm}$) radiation as the source at a rate of 2°/min and with 1° glancing angle against the incident beam on the specimen surface.

Note 2: The dried specimen for SEM observation should be thinly metal-coated to induce electro conductivity. The SEM photos should be taken both at high magnifications (around 10,000) and low magnifications (around 1000).

Note 3: The TF-XRD measurement can clearly identify the apatite formation on the specimen. The SEM observation can observe the material formation on the specimen, but can not identify whether the formed material is apatite or not. Therefore, the SEM observation should be accompanied with TF-XRD measurement. However, formed apatite grains and layers have characteristic features to be identified, and the apatite formation is sometimes estimated only on SEM.

References

- [1] Hench LL, Splinter RJ, Allen WC, Greenlee TK. Bonding mechanisms at the interface of ceramics prosthetic materials. *J Biomed Mater Res* 1972;2:117–41.
- [2] Jarcho M, Kay JI, Gummaer RH, Drobeck HP. Tissue, cellular and subcellular events at a bone–ceramic hydroxyapatite interface. *J Bioeng* 1977;179–92.
- [3] Rejda BJ, Peelen GJG, de Groot K. Tricalcium phosphate as a bone substitute. *J Bioeng* 1977;1:93–7.
- [4] Legeros RZ, Lin S, Rohanizadeh R, Mijares D, Legeros JP. Biphasic calcium phosphate bioceramics: preparation, properties and applications. *J Mater Sci Mater Med* 2003;14:201–9.
- [5] Kokubo T, Shigematsu M, Nagashima Y, Tashiro M, Nakamura T, Yamamuro T, et al. Apatite- and wollastonite-containing glass-ceramic for prosthetic application. *Bull Inst Chem Res Kyoto Univ* 1982;60:260–8.
- [6] Kokubo T. Bioactive glass ceramics: properties and applications. *Biomaterials* 1991;12:155–63.
- [7] Ogino M, Ohuchi F, Hench LL. Compositional dependence of the formation of calcium phosphate films on bioglass. *J Biomed Mater Res* 1980;14:55–64.
- [8] Kitsugi T, Nakamura T, Yamamuro T, Kokubo T, Shibuya T, Takagi M. SEM-EPMA observation of three types of apatite-containing glass ceramics implanted in bone: the variance of a Ca, P-rich layer. *J Biomed Mater Res* 1987;21:1255–71.
- [9] Kokubo T, Ohtsuki C, Kotani S, Kitsugi T, Yamamuro T. Surface structure of bioactive glass-ceramic A–W implanted into sheep and human vertebra. In: Heimke G, editor. *Bioceramics*, vol. 2. Cologne: German Ceramic Society; 1990. p. 113–21.
- [10] Kokubo T, Kushitani H, Sakka S, Kitsugi T, Yamamuro T. Solutions able to reproduce in vivo surface-structure change in bioactive glass-ceramic A–W. *J Biomed Mater Res* 1990;24:721–34.
- [11] Kokubo T, Ito S, Huang T, Hayashi T, Sakka S, Kitsugi T, et al. Ca, P-rich layer formed on high-strength bioactive glass-ceramic A–W. *J Biomed Mater Res* 1990;24:331–43.
- [12] Filgueiras MR, Torre GL, Hench LL. Solution effects on the surface reactions of a bioactive glass. *J Biomed Mater Res* 1993;27:445–53.
- [13] Ohtsuki C, Aoki Y, Kokubo T, Bando Y, Neo M, Nakamura T. Transmission electron microscopic observation of glass-ceramic A–W and apatite layer formed on its surface in a simulated body fluid. *J Ceram Soc Japan* 1995;103:449–54.
- [14] Kitsugi T, Yamamuro T, Nakamura T, Kokubo T. The bonding of glass ceramics to bone. *Int Orthop* 1989;13:199–206.
- [15] Gamble JE. *Chemical anatomy, physiology and pathology of extra-cellular fluid*. Cambridge, MA: Harvard University Press; 1967. p. 1–17.
- [16] Ohtsuki C, Kushitani H, Kokubo T, Kotani S, Yamamuro T. Apatite formation on the surface of Ceravital-type glass-ceramic in the body. *J Biomed Mater Res* 1991;25:1363–70.
- [17] Neuman W, Neuman M. *The chemical dynamics of bone mineral*. IL: University of Chicago; 1958. p. 34.
- [18] Cho S, Nakanishi K, Kokubo T, Soga N, Ohtsuki C, Nakamura T, et al. Dependence of apatite formation on silica gel on its structure: effect of heat treatment. *J Am Ceram Soc* 1995;78:1769–974.
- [19] Oyane A, Kim HM, Furuya T, Kokubo T, Miyazaki T, Nakamura T. Preparation and assessment of revised simulated body fluids. *J Biomed Mater Res* 2003;65A:188–95.
- [20] Oyane A, Onuma K, Ito A, Kim HM, Kokubo T, Nakamura T. Formation and growth of clusters in conventional and new kinds of simulated body fluids. *J Biomed Mater Res* 2003;64A:339–48.
- [21] Takadama H, Hashimoto M, Mizuno M, Kokubo T. Round-robin test of SBF for in vitro measurement of apatite-forming ability of synthetic materials. *Phos Res Bull* 2004;17:119–25.
- [22] Anderson ÖH, Karlsson KH. On the bioactivity of silicate glass. *J Non-Cryst Solids* 1991;129:145–51.
- [23] Neo M, Kotani S, Nakamura T, Yamamuro T, Ohtsuki C, Kokubo T, et al. A comparative study of ultrastructures of the interfaces between four kinds of surface-active ceramic and bone. *J Biomed Mater Res* 1992;26:1419–32.
- [24] Höland W, Vogel W, Naumann K. Interface reaction between machinable bioactive glass-ceramics and bone. *J Biomed Mater Res* 1985;19:303–12.
- [25] Kokubo T, Kushiyani M, Ebisawa Y, Kitsugi T, Kotani S, Oura K, et al. Apatite formation on bioactive ceramics in body environment. In: Oonishi, Aoki H, Sawai K, editors. *Bioceramics*. Tokyo: Ishiyaku EuroAmerica; 1988. p. 157–62.
- [26] Kim HM, Himeno T, Kawashita M, Kokubo T, Nakamura T. The mechanism of biomineralization of bone-like apatite on synthetic hydroxyapatite: an in vitro assessment. *J R Soc Interface* 2004;1:17–22.
- [27] Chan H, Mijares D, Ricci JL. In vitro dissolution of calcium sulfate: evidence of bioactivity. *Transactions of the seventh world biomaterials congress*, 2004. p. 627.
- [28] Judasz JA, Best SM, Bonfield W, Kawashita M, Miyata N, Kokubo T, et al. Apatite-forming ability of glass-ceramic apatite-wollastonite-polyethylene composites: effect of filler content. *J Mater Sci: Mater Med* 2003;14:489–95.
- [29] Judasz JA, Ishii S, Best SM, Kawashita M, Neo M, Kokubo T, et al. Bone-bonding ability of glass-ceramic apatite-wollastonite-polyethylene composites. *Transactions of the seventh world biomaterials congress*, 2004. p. 665.
- [30] Ohtsuki C, Kokubo T, Neo M, Kotani S, Yamamuro T, Nakamura T, et al. Bone-bonding mechanism of sintered β -3CaO-P₂O₅. *Phos Res Bull* 1991;1:191–6.
- [31] Ohtsuki C, Aoki Y, Kokubo T, Fujita Y, Kotani S, Yamamuro T. Bioactivity of limestone and abalone shell. *Transactions of the 11th annual meeting of Japanese Society for Biomaterials*, 1989. p. 12.
- [32] Kotani S, Fujita Y, Kitsugi T, Nakamura T, Yamamuro T. Bone bonding mechanism of β -tricalcium phosphate. *J Biomed Mater Res* 1991;25:1303–15.
- [33] Neo M, Nakamura T, Ohtsuki C, Kokubo T, Yamamuro T. Apatite formation of three kinds of bioactive materials at early stage in vivo: a comparative study by transmission electron microscopy. *J Biomed Mater Res* 1993;27:999–1006.

- [34] Fujita Y, Yamamuro T, Nakamura T, Kotani S. The bonding behavior of calcite to bone. *J Biomed Mater Res* 1991;25:991–1003.
- [35] Fujita Y, Yamamuro T, Nakamura T, Kotani S, Kokubo T, Ohtsuki C. The bonding behavior of limestone and abalone shell to bone. *Transactions of the 11th annual meeting of Japanese Society for Biomaterials*, 1989. p. 3.
- [36] Kim HM, Miyaji F, Kokubo T, Ohtsuki C, Nakamura T. Bioactivity of Na_2O – CaO – SiO_2 glasses. *J Am Ceram Soc* 1995;78:2405–11.
- [37] Fujibayashi S, Neo M, Kim HM, Kokubo T, Nakamura T. A comparative study between in vivo bone growth and in vitro apatite formation on Na_2O – CaO – SiO_2 glasses. *Biomaterials* 2003;24:1349–56.
- [38] Oonishi H, Henchi LL, Wilson J, Sugihara F, Tsuji E, Matsuura M, et al. Quantitative comparison of bone growth behavior in granules of Bioglass(R), A–W glass-ceramic and hydroxyapatite. *J Biomed Mater Res* 2000;51:37–46.
- [39] Ohtsuki C, Kokubo T, Yamamuro T. Mechanism of apatite formation on CaO – SiO_2 P_2O_5 glasses in a simulated body fluid. *J Non-Cryst Solids* 1992;143:84–92.
- [40] Ebisawa Y, Kokubo T, Ohura K, Yamamuro T. Bioactivity of CaO – SiO_2 -based glasses: in vitro evaluation. *J Mater Sci Mater Med* 1990;1:239–44.
- [41] Ohura K, Nakamura T, Yamamuro T, Kokubo T, Ebisawa Y, Kotoura Y, et al. Bone-bonding ability of P_2O_5 -free CaO – SiO_2 glasses. *J Biomed Mater Res* 1991;25:357–65.
- [42] Ohura K, Nakamura T, Yamamuro T, Ebisawa Y, Kokubo T, Kotoura Y, et al. Bioactivity of CaO – SiO_2 glasses added with various ions. *J Mater Sci Mater Med* 1992;3:95–100.
- [43] Ebisawa Y, Miyagi F, Kokubo T, Ohura K, Nakamura T. Bioactivity of ferrimagnetic glass-ceramics in the system FeO – Fe_2O_3 – CaO – SiO_2 . *Biomaterials* 1997;18:1277–84.
- [44] Ohura K, Ikenaga M, Nakamura T, Yamamuro T, Ebisawa Y, Kokubo T, et al. A heat-generating bioactive glass-ceramic for hyperthermia. *J Appl Biomater* 1991;2:153–9.
- [45] Ikenaga M, Ohura K, Yamamuro T, Kotoura Y, Oka M, Kokubo T. Localized hyperthermic treatment of experimental bone tumors with ferromagnetic ceramics. *J Orthop Res* 1993;11:849–55.
- [46] Li P, Ohtsuki C, Kokubo T, Nakanishi K, Soga N, Nakamura T, et al. Apatite formation induced on silica gel in a simulated body fluid. *J Am Ceram Soc* 1992;75:2094–7.
- [47] Li P, Ohtsuki C, Kokubo T, Nakanishi K, Soga N, Nakamura T, et al. A role of hydrated silica, titania and alumina in forming biologically active bone-like apatite on implant. *J Biomed Mater Res* 1994;28:7–15.
- [48] Uchida M, Kim HM, Kokubo T, Nakamura T. Bonelike apatite formation induced on zirconia gel in simulated body fluid and its modified solutions. *J Am Ceram Soc* 2001;84:2041–4.
- [49] Miyazaki T, Kim HM, Kokubo T, Ohtsuki C, Kato H, Nakamura T. Apatite-forming ability of niobium oxide gels in a simulated body fluid. *J Ceram Soc Japan* 2001;109:929–33.
- [50] Miyazaki T, Kim HM, Kokubo T, Kato H, Nakamura T. Induction and acceleration of bonelike apatite formation on tantalum oxide gel in simulated body fluid. *J Sol-gel Sci Technol* 2001;21:83–8.
- [51] Kim HM, Miyaji F, Kokubo T, Nakamura T. Preparation of bioactive Ti and its alloys via simple chemical surface treatment. *J Biomed Mater Res* 1996;32:409–17.
- [52] Miyazaki T, Kim HM, Miyaji F, Kokubo T, Nakamura T. Bioactive tantalum metal prepared by NaOH treatment. *J Biomed Mater Res* 2000;50:35–42.
- [53] Takadama H, Kim HM, Kokubo T, Nakamura T. TEM-EDX study of mechanism of bonelike apatite formation on bioactive titanium metal in simulated body fluid. *J Biomed Mater Res* 2001;57:441–8.
- [54] Nishiguchi S, Fujibayashi S, Kim HM, Kokubo T, Nakamura T. Biology of alkali- and heat-treated titanium implants. *J Biomed Mater Res* 2003;67A:28–35.
- [55] Kato H, Nakamura T, Nishiguchi S, Matsusue Y, Kobayashi M, Miyazaki T, et al. Bonding of alkali- and heat-treated tantalum implant to bone. *J Biomed Mater Res (Appl Biomater)* 2000;53:28–35.

Clin Orthop in press

The Frank Stinchfield Award

Grafting of Biocompatible MPC Polymer on Cross-linked Polyethylene Liner Surface for Extending Longevity of Artificial Hip Joints

*Toru Moro, MD**; *Yoshio Takatori, MD**; *Kazuhiko Ishihara, PhD†*; *Kozo Nakamura, MD**; *and Hiroshi Kawaguchi, MD**

*Department of Sensory & Motor System Medicine, Faculty of Medicine, †Department of Materials Engineering, School of Engineering, The University of Tokyo, Hongo 7-3-1, Bunkyo, Tokyo 113-0033, Japan.

Correspondence to: Toru Moro, MD, PhD.

Department of Sensory & Motor System Medicine, Faculty of Medicine,
The University of Tokyo, Hongo 7-3-1, Bunkyo, Tokyo 113-0033, Japan.

Phone: +81-3-5800-8656

Fax: +81-3-3818-4082

E-mail: moro-ort@h.u-tokyo.ac.jp

ABSTRACT

Aseptic loosening induced by wear particles from the polyethylene (PE) liner is the most serious complication associated with total hip replacement. We prepared a novel hip PE liner with the surface graft of a novel biocompatible phospholipid polymer, 2-methacryloyloxyethyl phosphorylcholine (MPC), and reported that the grafting decreased the production of wear particles during a short term and the subsequent bone resorptive responses. For the clinical application, the present study investigated the stability of the MPC grafting by the sterilization procedure and the wear resistance of the sterilized liner during longer loading comparable to clinical usage. Radiological spectroscopy analyses confirmed the stability of the MPC polymer on the liner surface after the gamma irradiation. A hip joint wear simulator trials up to 1.0×10^7 cycles using the sterilized cross-linked polyethylene liners with and without MPC grafting (CLPE and MPC-CLPE) revealed that the MPC grafting markedly decreased the friction, the production of wear particles, and the wear of the liner surface. This study demonstrated a marked improvement of wear resistance of the PE liner by the MPC grafting for clinically comparative periods even after the sterilization procedure, indicating that MPC grafting is a promising technology for extending longevity of artificial hip joints.

INTRODUCTION

The incidence of osteoarthritis and rheumatoid arthritis is on the rise due to the worldwide growth of elderly populations. Total hip replacement is one of the most successful and effective treatments for the end-stage patients with arthritic diseases affecting the hip joint.^{5, 37} The number of primary total hip replacements performed annually is estimated to be more than 1.3 million world-wide with 50-140 operations / 100,000 inhabitants in North American, European and Australian countries, and this is expected to continue to increase over at least the next three decades.^{1, 25, 33} Despite improvements in implant design and surgical technique, periprosthetic osteolysis causing aseptic loosening of artificial joints remains as the most serious problem limiting their survivorship and clinical success.²¹ Up to 20% of patients with total hip replacement develop radiographic evidence of aseptic loosening within 10 years³, about half of whom require revision surgery due to pain and loss of function. However, there is no therapeutic intervention of the loosening other than the revision surgery, and the number of salvage operations whose outcomes are much poorer than the primary ones is also increasing.²⁹

Pathogenesis of the periprosthetic osteolysis is known to be a consequence of the host inflammatory response to wear particles originating from the prosthetic devices.²¹ The most abundant and bone resorptive particle within the periprosthetic tissues is polyethylene (PE) generated from the interface between the PE and metal components³⁰, which induces the phagocytosis by macrophages and the following secretion of bone resorptive cytokines.⁹ Hence, there are two approaches to prevent aseptic loosening; one is to reduce the amount of PE wear particles and the other is to suppress the subsequent bone resorptive responses. A number of studies have been performed to increase the wear resistance of PE or to develop alternative bearing surfaces other than PE; however, none has fully solved the problem yet.

Recent observations of the healthy human articular cartilage surface have disclosed that it is covered with a nanometer-scaled phospholipid layer that improve the lubricity and biocompatibility of the articulating surface.^{13, 24} Hence, grafting a polymer including the biocompatible phospholipid-like layer on the liner surface may realize the interface conditions that are similar to healthy physiological joints. The 2-methacryloyloxyethyl phosphorylcholine (MPC) polymer is our original biocompatible polymer whose side chain is composed of phosphorylcholine resembling phospholipids of biomembrane (Fig. 1).²⁰ The MPC grafting onto the surface of other medical devices has already been shown to suppress biological reactions even when they are in contact with living organisms^{19, 42}, and is now clinically used on the surfaces of intravascular stents, intravascular guide wires, soft contact lenses and the artificial lung under the authorization of the Food and Drug Administration (FDA) of United States.^{23, 27} Aiming at the reduction of the wear particles and the elimination of periprosthetic osteolysis, we prepared a novel hip PE liner with MPC grafted onto its surface. Our recent study on the mechanical and biological effects of MPC revealed that the grafting decreased the production of wear particles during a short term up to 3×10^6 cycles in the hip joint wear simulator and the bone resorptive responses: secretion of cytokines and osteoclastogenesis.³⁴ However, the effect of sterilization procedure on the stability of the MPC grafting and the wear resistance of the sterilized liner during longer loading comparable to clinical usage remain to be elucidated before it is ready for clinical application. The present study therefore investigated the MPC stability after the sterilization, and the wear resistance of the sterilized MPC-grafted PE liner during 1×10^7 cycles of loading, that is comparable to 10-30 years of physical walking, in the hip joint simulator.

MATERIALS AND METHODS

Materials

MPC was synthesized and purified as previously reported.²⁰ The chemical structure of the MPC is shown in Fig 1. Cross-linked PE (CLPE) liner (K-MAX Excellink[®]) and cobalt-chromium-molybdenum alloy femoral heads (K-MAX[®]HH-02,) were obtained from Japan Medical Materials Corporation (Osaka, Japan). Grafting of the MPC polymer onto the surfaces of the CLPE liner was performed by a photoinduced polymerization technique as previously reported.^{16, 34} Briefly, CLPE liners were placed in the MPC solution (0.5 mol/L) and photoinduced polymerization on the liner surface was carried out using an ultra-high pressure mercury lamp (UVL-400HA, Riko-Kagaku Sangyo Co. Ltd., Chiba, Japan).

Analysis of PE surface

In order to evaluate the influence of sterilization procedure, MPC grafted CLPE plates (MPC-CLPE plates) were sterilized with gamma irradiation (2.5 Mrad) in nitrogen as conventionally used. Elemental analysis at the surface was carried out with a highly sensitive X-ray photoelectron spectroscopy (XPS; PHI5400MC, Perkin Elmer Inc., Wellesley, MA), a fourier-transform infrared spectroscopic (FT-IR) analyzer (Perkin-Elmer FT-IR 1650, *ibid*), and a transmission electron microscope (TEM; JEM-1010 Japan Electron Optics Laboratory Co., Ltd, Tokyo, Japan). The contact angle of water on the CLPE surface was measured by the sessile drop method at room temperature (22°C) using a goniometer (Erma G-1, Tokyo, Japan).¹⁸ At least ten contact angles were measured and averaged.

Hip joint wear simulator experiment

A 12-station hip simulator apparatus (MTS, MTS Systems Co. Ltd., Minneapolis, MN) with two kinds of gamma sterilized CLPE liners in 46 mm acetabular cups: a CLPE liner and an MPC-grafted CLPE liner (MPC-CLPE liner), coupled to 26 mm cobalt-chromium-molybdenum alloy heads were mounted on the rotating blocks to produce a biaxial or orbital motion. Friction torque between the liner and the femoral head was measured using a torque measuring instrument (Original machine, Kobe Steel, Co.,Ltd.). A Paul-type loading profile which is a physiological walking simulation with continuous cyclic motion and loading was applied (maximum force; 280 kgf, frequency; 1 Hz).³⁸ A diluted bovine calf serum (25%) in distilled water was used as the lubricant. Sodium azide (10 mL/L) and EDTA (20 mM) were added to prevent microbial contamination and minimize calcium phosphate formation on the implant surface. The simulator was run up to 1×10^7 cycles for 8 months. At intervals of 5×10^5 cycles the liners were removed from the simulator and weighed on a microbalance (Sartorius GENIUS ME215S, Sartorius AG, Goettingen, Germany). The lubricant was collected and stored at -20°C for further analysis. After the total loading, microdamage of the liner surface was measured by a 3-dimensional coordinate measuring machine (XYZAX GS800B, Tokyo Seimitsu Co., Ltd., Tokyo, Japan). To evaluate true removal of material caused by wear, melt-recovery experiments were performed and the the liner surface was analyzed with confocal scanning laser microscope (OLS1200, Olympus Corp., Tokyo, Japan) as previously reported.³⁵ For the femoral head surface, in addition to scanning electron microscopy (SEM) evaluation, the surface roughness value R_a was measured using a roughness measuring instrument (SURFTEST-501, Mitsutoyo Co., Ltd., Kanagawa, Japan) with a 5 μ m diameter contact probe. For the isolation of wear particles, the lubricant after the loading was incubated with 5 N NaOH solution in order to digest adhesive proteins that were degraded and precipitated; the particles were then collected

and underwent sequential filtrations, as previously reported.²² The size of particles was defined as the maximum dimensions by the SEM analysis.

Statistical Analysis

Means of groups were compared by ANOVA and significance of differences was determined by post-hoc testing using Bonferroni's method.

RESULTS

The stability of the MPC polymer on MPC-CLPE plate after the gamma irradiation was confirmed using XPS and FT-IR spectroscopy. The XPS signals indicating nitrogen atom (N_{1s}) at 402 eV and phosphorus atom (P_{2p}) at 135 eV, which are attributable to the phosphorylcholine group in the MPC unit, were observed on the MPC-CLPE plate after gamma irradiation (Fig 2A). The FT-IR transmittance absorption representing phosphate group (P-O) at 1240, 1080 and 970 cm^{-1} , and ketone group (C=O) at 1720 cm^{-1} was also observed even after the grafting and irradiation (Fig 2B). The contact angle of a water drop on the MPC-CLPE plate was 12.3 ± 2.4 degrees while that of the original CLPE plate was 89.9 ± 2.9 degrees (Fig 2C), suggesting that hydrophobic CLPE surface was kept covered with hydrophilic MPC polymer even after the gamma irradiation.

Mechanical effects of the MPC grafting on the hip prosthesis were examined using a hip joint wear simulator²² (Fig. 3A) under the conditions recommended by the International Organization for Standardization (ISO). We prepared CLPE liners with photoinduced grafting of MPC onto their surface (MPC-CLPE liner), and compared them with CLPE liners without the MPC grafting (CLPE liner). The friction torques of the two liners against the femoral head were compared before the loading test. The average friction torque was about 80% lower in MPC-CLPE liners than CLPE liners (Fig 3B). The gravimetric analysis showed a total weight loss of 34.7 ± 2.5 mg in CLPE liners after the 1×10^7 cycles of loading (Fig 3C). In contrast, MPC-CLPE liners continued to gain weights, and showed a total weight gain of 8.7 ± 1.0 mg, which might have been due to water absorption into the liner from the lubricant.

Three-dimensional morphometric analyses of MPC-CLPE liner surface revealed no or very little wear, while substantial wears were detected in CLPE liners (Fig 4A). The confocal scanning laser microscopic analysis of the liner surface revealed that the original machine marks that are clearly visible before the loading still remained on the MPC-CLPE liner surface, although they were completely obliterated on the CLPE liner (Fig. 4B). The XPS analysis also confirmed the remainder of the specific spectra of N_{1s} and P_{2p} on the MPC-CLPE liner surface just as in Fig 2A even after the loading (data not shown), indicating that the MPC-CLPE grafting was maintained even after the loading of 1×10^7 cycles. The femoral heads were free of visible scratches and the surface roughness expressed by the R_a values was not different between before and after the loading in both groups ($R_a=0.04-0.05$ μm), suggesting that there was no abrasive contamination with metal particles from the heads in the hip joint simulator (Fig. 4C).

The SEM analysis of the wear particles isolated from the lubricants revealed no significant difference in the particle shape or size between CLPE and MPC-CLPE liners. Most of the particles from both liners were ranged from 0.1-1.0 μm in size with round or spindle shape (Fig. 5).

DISCUSSION

The present study demonstrated that our original biocompatible phospholipid polymer MPC grafting onto the PE liner surface of the hip prosthesis markedly decreased the friction and the production of wear particles during 1×10^7 cycles of loading in the hip joint simulator. Since PE particles are known to be most abundant and catabolic among wear particles in the periprosthetic tissues³⁰, alternative bearing surfaces have been proposed such as ceramic-on-ceramic and metal-on-metal articulations; however, these have their own potential disadvantages.^{2,4} The long history and popularity of PE as a bearing surface has led to research in the development of tougher and more wear resistant PE materials: the incorporation of short chopped carbon fibers in PE matrix (Poly IITM)^{7,41}, the extension of chain crystallite morphology with thicker lamellae and higher crystallinity (HylamerTM)²⁸, and the creation of a three-dimensional molecular network by the cross-linking. Among them, only the cross-linking most efficiently improved the wear resistance and suppressed the periprosthetic osteolysis in the clinical setting.³¹ It is therefore noteworthy that the MPC grafting onto the CLPE surface further increased the wear resistance over the conventional CLPE. Since the 1×10^7 cycles of loading in the hip simulator is comparable to 10-30 years of physical walking in the hip joint simulator, the MPC grafting is likely to extend the longevity of the artificial hip joints at least 10 years.

Clinical and laboratory research has revealed that sterilization methods can dramatically affect the *in vivo* performance of PE liners.³² At present, PE liners can be sterilized with gamma irradiation, gas plasma, or ethylene oxide. Gamma sterilization in air has been shown to lead to oxidation of the PE and adversely affect its mechanical properties. In the mid 1990s, the use of gamma sterilization in air was replaced by gamma sterilization in an inert environment, such as nitrogen, argon, or vacuum. In this study, we used CLPE liners, sterilized gamma irradiation in nitrogen, and revealed that the sterilization method did not affect the property of MPC grafting with respect to surface analysis and hip joint simulator study. In fact, other MPC-grafted medical devices such as oxygenator, the intravascular stents, the intravascular guide wires are sterilized with gamma irradiation or ethylene oxide. Moreover, the MPC polymer has good thermal resistance and could be processed by heat treatment at 150°C, and our preliminary study showed that gas plasma and ethylene oxide sterilization did not affect its properties.³⁶

With respect to the reduction of wear by the MPC grafting, we should consider the lubrication mechanism between the liners and metal heads of the hip joint simulator. Although phospholipids themselves are known to work as effective boundary lubricants^{12,40}, recent studies of natural synovial joints have shown that fluid film lubrication by the intermediate hydrated layer is the predominant mechanism under physiological walking conditions.⁸ Since the present study revealed that the MPC grafting onto the CLPE plate increased the hydrophilicity and our previous study showed that the free water fraction on the MPC polymer surface is kept at a higher level¹⁷, the reduction of wear is likely to arise from the hydrated lubricating layer that is formed by the MPC grafting.

In addition to the improvement of the wear resistance of the liner, it is also important to decrease bone resorptive responses induced by wear particles. Substantial differences between the wear particles from cross-linked and non-cross-linked PE liners have been found *in vitro*. The CLPE liner releases a relatively high number of submicrometer and nanometer-sized PE particles and relatively fewer particles that are several micrometers in dimension.¹¹ These submicrometer-sized PE particles induce a greater inflammatory response *in vitro* than larger particles.¹⁵ Hence, the biological activity of PE particles will be dependent not only upon the total volume of wear or the number of particles generated, but also upon the proportion of those

particles which are within the most biologically active size range. In our previous study, MPC nanoparticles (500 nm in diameter) were used in murine particle-induced osteolysis model to investigate the biocompatibility of these particles.³⁴ *In vitro* culture systems revealed that MPC nanoparticles were hardly phagocytosed by macrophages and did not induce the production of bone resorptive cytokines. Furthermore, the culture medium of macrophages exposed to MPC nanoparticles did not induce osteoclast formation from bone marrow cells. These results suggest that MPC particles are biologically inert in respect to phagocytosis by macrophages and subsequent bone resorptive actions. There is an increasing number of studies that address the potential pharmacologic modification of the adverse host response to wear particles^{6, 10}, such as cytokine antagonists, cyclooxygenase-2 inhibitors, and osteoprotegerin or anti-RANKL antibody; however, they may cause serious side effects since the agents should be taken for a long period after surgery. Because the lack of side effects of the MPC polymer grafting has already been confirmed clinically by several biomaterials^{23, 26}, this grafting surpasses the developing pharmacologic treatments.

Although this study focused on the hip prosthesis whose loosening is the most frequent and serious among total joint replacements of upper and lower extremities, the MPC polymer grafting can be applicable to the prevention of periprosthetic osteolysis of other joints, in which PE particles from articular interfaces between the PE and metal components are also thought to initiate the catabolic cascade.^{14, 39} From the advantages shown in this study, we believe that the MPC polymer grafting will make a significant improvement in total joint replacements by preventing periprosthetic osteolysis and aseptic loosening. The development of this nanotechnology would improve the quality of care of patients having total joint replacement and have a substantial public health impact. We are now designing a large-scale clinical trial.

ACKNOWLEDGEMENTS

We thank Tomohiro Konno, Noboru Yamawaki, Takatoshi Miyashita, Masayuki Kyomoto, Hiroaki Takadama, Kaori Jono, and Reiko Yamaguchi for their excellent technical help. This work was supported by Grants-in-Aid for Scientific Research from the Japanese Ministry of Education, Culture, Sports, Science and Technology (#15390449), and Health and Welfare Research Grant for Traslationalresearch from the Japanese Ministry of Health, Labour and Welfare.